Realization of a Room-Temperature Spin Dynamo: The Spin Rectification Effect

Y. S. Gui, N. Mecking, X. Zhou, Gwyn Williams, and C.-M. Hu*

Department of Physics and Astronomy, University of Manitoba, Winnipeg, Canada R3T 2N2

(Received 18 October 2006; published 9 March 2007)

We demonstrate a room-temperature spin dynamo where the precession of electron spins in ferromagnets converts energy from microwaves to a bipolar current of electricity. The current/power ratio is at least 3 orders of magnitude larger than that found previously for spin-driven currents in semiconductors. The observed bipolar nature and intriguing symmetry are fully explained by the spin rectification effect via which the nonlinear combination of spin and charge dynamics creates dc currents.

DOI: 10.1103/PhysRevLett.98.107602 PACS numbers: 76.50.+g, 73.50.Pz, 84.40.−x, 85.75.−d

There is currently great interest in generating dc currents via spin dynamics [1–4]. The significance is twofold: On the one hand, it provides electrical means for investigating spin dynamics, while on the other hand, it may pave the way for designing new spin sources for spintronic applications. In semiconductor materials with spin-orbit coupling, both aspects have been demonstrated [3–5]. Progress with ferromagnetic metals (FM) has been achieved using magnetic multilayers [1,2]. Very recently, a few groups [6,7] have begun to develop techniques for electrical detection of spin resonances in a FM single layer. Understanding the dc effects in a FM single layer is crucial for clarifying whether spin pumping effects might exist in magnetic multilayers [7,8]. Until now, in contrast to the case for semiconductors [3,4], the important question of how to effectively generate dc currents from a single FM remained unclear. This leaves our understanding of the interplay between spin dynamics and electrostatic response incomplete, as evidenced in the different views represented in recent work [7,8].

In this Letter, we present both experimental and theoretical answers to this question. A spin dynamo is constructed which generates dc currents via spin dynamics. The observed bipolar nature and intriguing symmetry allow us to unambiguously identify the origin of this phenomenon as the spin rectification effect. To give a simple picture, we begin with the well-known optical rectification effect, which occurs in nonlinear media with large second-order susceptibility. Here the optical response to the product of time-dependent electric fields $e_0 \cos(\omega t)$ is governed by the trigonometric relation: $\cos(\omega_1 t)\cos(\omega_2 t) = \{\cos[(\omega_1 - \omega_2)t] + \cos[(\omega_1 + \omega_2)t]\}/2$. If the frequencies $\omega_1 = \omega_2$, the terms with difference and sum frequencies cause optical rectification and second harmonic generation, respectively. A similar nonlinear dynamic response to the product of rf electric and magnetic fields is the origin of the spin rectification effect, investigated here by using a spin dynamo.

The spin dynamo we constructed is sketched in Figs. 1(b) and 1(c). It is the microscopic counterpart of Faraday's dynamo, shown in Fig. 1(a). Both devices generate dc currents in a static magnetic field, but the rotational motion of a macroscopic copper plate in Faraday's dynamo is replaced by microscopic spin precession in the spin dynamo. The device is based on a Permalloy (Py) microstrip (typically 2.45 mm × 20 μm × 137 nm) placed in the slot between the ground and signal strips of a coplanar waveguide (CPW) [9]. From anisotropic magnetoresistance (AMR) and ferromagnetic resonance (FMR) measurements, the following material parameters have been determined for the Py strip: the conductivity $\sigma = 3 \times 10^4\ \Omega^{-1}\,\mathrm{cm}^{-1}$, the magnetoanisotropy $\Delta\rho/\rho = 0.019$, the saturation magnetization $\mu_0 M_0 = 1.0$ T, and the demagnetization factors $N_x \approx 0$, $N_y \approx 0.007$, and $N_z \approx 0.993$. Here μ_0 is the permeability of vacuum. The coordinate system is shown in Fig. 1(c). The CPW is deposited with Au/Ag/Cr layers (5/550/5 nm) on top of a semi-insulating GaAs substrate and is impedance matched to 50 Ω. The dimensions of the CPW are 150 and 100 μm in width for the strips and the slots, respectively. As sketched in Fig. 1(b), by setting the device in an electromagnet and feeding the CPW with microwaves using a conventional microwave power generator, dc currents

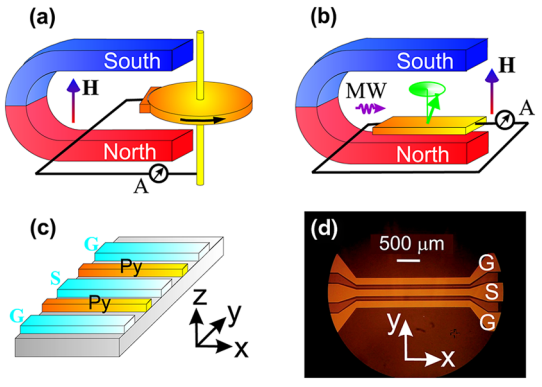

FIG. 1 (color online). (a) Faraday's dynamo with a revolving copper disk converts energy from rotation to a current of electricity. (b) Spin dynamo with a FM strip converts energy from spin precession to a bipolar current of electricity. (c) Diagram of the spin dynamo structure with Py strips placed in slots between the ground (G) and signal (S) lines of a coplanar waveguide. (d) Top view micrograph of a device.

are generated in the Py strip at room temperature. To preserve the symmetry of the CPW, two identical Py microstrips are inserted in both slots. They are measured independently, and the same effect is found. Several spin dynamos with different Py thicknesses have been measured in various configurations. The data reported here have been rendered, both experimentally and theoretically, to convey the most significant aspects of the observed phenomena. For the same purpose, a special sample holder has been constructed that enables the spin dynamo to rotate about both the x and the y axes with an angular resolution approaching 0.01°.

Figure 2 demonstrates the production of bipolar dc currents. The microwave frequency is set at 5.4 GHz. The current I flowing along the x axis is measured using a current amplifier while sweeping the magnetic field H applied nearly perpendicular to the Py strip. We define α and β as the small angles of the field direction tilted away from the z axis towards the x and y axes, respectively. As shown in Fig. 2(a), when β is set to zero, the current $I(\alpha, H)$ measured at $\alpha = -1°$ shows a positive peak and a negative dip. The current rapidly diminishes when α is tuned to zero and then changes polarity when α becomes positive [Fig. 2(b)]. The same bipolar behavior holds true for the current $I(\beta, H)$ measured at $\alpha = 0$ and plotted in Figs. 2(c) and 2(d), except that its polarity also changes upon reversing the direction of the applied magnetic field. In addition, the sharp features in Figs. 2(a) and 2(b) disappear in Figs. 2(c) and 2(d). The insets in Fig. 2 summarize the angular dependence of the maximum bipolar current, measured by using standard lock-in techniques to enhance the signal/noise ratio at extremely small angles.

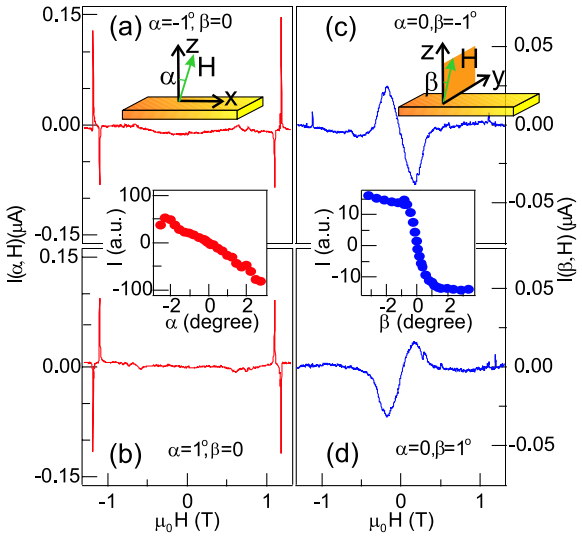

FIG. 2 (color online). Bipolar dc currents measured as a function of the magnetic field H applied with angles (a) $\alpha = -1°$, $\beta = 0$, (b) $\alpha = 1°$, $\beta = 0$, (c) $\alpha = 0$, $\beta = -1°$, and (d) $\alpha = 0$, $\beta = 1°$. The microwave frequency is fixed at 5.4 GHz. The insets summarize the angular dependence of the maximum current measured at $H < 0$.

The curious results of Fig. 2 can be summarized with the following observed bipolar symmetry:

$$I(\alpha, H) = -I(-\alpha, H) = I(\alpha, -H) \quad \text{for } \beta = 0;$$
$$I(\beta, H) = -I(-\beta, H) = -I(\beta, -H) \quad \text{for } \alpha = 0. \tag{1}$$

The sharp features in the $I(\alpha, H)$ trace suggest a resonant nature, which is confirmed by frequency dependence measurements. At higher frequencies, up to four resonances are observed. For $|H| > M_0$, the measured resonant relations, plotted in Fig. 3(a), follow the dispersion of standing spin waves (SSW) in Py films [10], given by $\omega = \gamma(|H| - M_0 + 2Ak^2/\mu_0 M_0)$. Here $k = p\pi/d$ is the wave vector with the values of p determined by the number of half-wavelengths in the Py strip with a thickness d. The solid lines in Fig. 3(a) are calculated using a gyromagnetic ratio $\gamma = 181\mu_0$ GHz/T and an exchange constant $A = 1.22 \times 10^{-11}$ N for Py [10]. Four modes with $p = 0$, 2, 3, and 4 are determined from the observed resonances, which indicates an intermediate pinning condition [11]. With $|H| < M_0$, the dispersion for SSW was previously unclear, due partially to the experimental challenge of detecting spin waves in a single Py microstrip. However, a similar field curve with a sharp cusp corresponding to the magnetic anisotropy was observed for the FMR [12]. Here, in the situation with $\beta = 0$, $\mathbf{M}$ rotates with increasing H from the easy axis parallel to the x axis towards the direction of $\mathbf{H}$. When α is small, we find that the solution of the magneto-

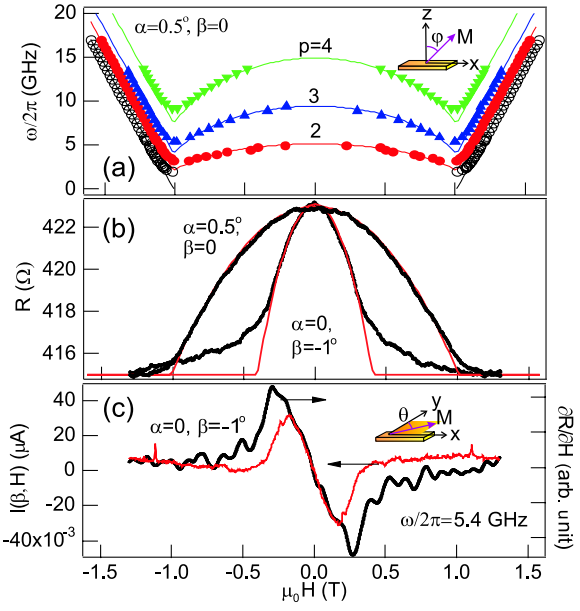

FIG. 3 (color online). (a) The measured frequency variation (marks) of the resonant features in the $I(\alpha, H)$ trace in comparison with the calculated dispersions (solid curves) for SSW. (b) AMR trace $R(H)$ measured (thick curves) and calculated (thin curves) at $\alpha = 0.5°$, $\beta = 0$ and $\alpha = 0$, $\beta = -1°$. (c) Current trace $I(\beta, H)$ measured at $\alpha = 0$, $\beta = -1°$ and 5.4 GHz (thin curve) in comparison with the field derivative of the AMR trace $\partial R(H)/\partial H$ (thick curve).

static problem gives $\cos\varphi \approx H\cos\alpha/M_0$, where the angle φ shown in Fig. 3(a) describes the direction of $\mathbf{M}$ with respect to the hard z axis. This simple relation is confirmed by the AMR measured at $\beta = 0$, plotted in Fig. 3(b), which is well represented by $R(H) = R(\infty)[1 + (\Delta\rho/\rho)\sin^2\varphi]$. By noticing the apparent similarity between the measured SSW dispersion and the AMR trace shown in Figs. 3(a) and 3(b), respectively, we suggest an empirical expression describing the SSW at $|H| < M_0$, given by $\omega = 2\gamma(Ak^2/\mu_0 M_0)\sqrt{1 + (4\pi/p)\sin^2\varphi}$, which well describes the measured dispersions.

It follows, therefore, that the spin dynamo is an ideal device for electrically detecting spin excitations in FM microstructures. In order to focus on the characteristics of the spin rectification effect, we leave the interesting physics of the spin excitation to a later paper and continue here by studying $I(\beta, H)$ measured at $\alpha = 0$. Since $\mathbf{H}$ in this case is tilted towards the y axis by a small angle β, and because $N_x \ll N_y \ll N_z$ for the long Py strip, we make an approximation to simplify the otherwise complicated magnetostatic problem. With increasing H, we assume $\mathbf{M}$ rotates first from the easy x axis towards the y axis before it moves out of the xy plane towards the direction of $\mathbf{H}$. Physically, this means the Py strip is much easier to magnetize along the y axis than the z axis. By describing the direction of $\mathbf{M}$ with the angle θ measured with respect to the y axis as shown in Fig. 3(c), we find $\cos\theta = H/M_1$ for $|H| < M_1$, and $\theta \approx 0$ for $|H| > M_1$, where $M_1 \equiv N_y M_0/\sin\beta$. As shown in Fig. 3(b), our approximation is justified by the AMR trace measured at $\alpha = 0$ and $\beta \approx -1°$, which agrees well with the curve calculated from $R(H) = R(\infty)[1 + (\Delta\rho/\rho)\sin^2\theta]$ for $|H| < M_1 \approx 0.4$ T. In this field range, we find that the current $I(\beta, H)$ partially follows $\partial R(H)/\partial H$. This comparison is shown in Fig. 3(c).

All of these results indicate that the current is induced by the dynamics of $\mathbf{M}$, as demonstrated by the following arguments on the nature of the spin rectification effect.

Under internal magnetic ($\mathbf{H}_i$) and electric ($\mathbf{E}$) fields, the magnetostatic response of the Py strip is determined by $\mathbf{M} = \hat{\chi}_0\mathbf{H}_i$ via the static permeability tensor $\hat{\chi}_0$, while the electrostatic response is described [13] by the generalized Ohm's equation $\mathbf{J} = \sigma\mathbf{E} - R_A(\mathbf{J}\cdot\mathbf{M})\mathbf{M} + \sigma R_0\mathbf{J}\times\mathbf{H}_i + \sigma R_1\mathbf{J}\times\mathbf{M}$. This equation takes into account spin-charge coupling effects phenomenologically via the nonlinear terms. Here the second term describes magnetoanisotropy via the AMR coefficient $R_A = \Delta\rho/\rho M_0^2$, which we have used to calculate the AMR trace $R(H)$. The last two terms describe the Hall effect with the ordinary and extraordinary Hall coefficients given by $R_0 = -1.9\times10^{-8}\ \Omega\,\mathrm{cm/T}$ and $R_1 \approx 3.3\times10^{-8}\ \Omega\,\mathrm{cm/T}$, respectively [14]. Dynamic responses of the Py strip to the rf magnetic ($\mathbf{h}$) and electric ($\mathbf{e}$) fields are given by $\mathbf{m} = \hat{\chi}\mathbf{h}$ and $\mathbf{j} = \hat{\sigma}\mathbf{e}$, respectively. Here the high-frequency permeability and conductivity tensors $\hat{\chi}$ and $\hat{\sigma}$ determine the dynamic spin accumulation $\mathbf{m}$ and the eddy current $\mathbf{j}$, respectively. If static and dynamic fields coexist, the nonlinear effects couple not only the magneto and electric responses but also the static and dynamic ones. Solving the above equations self-consistently, we obtain the dc current $\mathbf{I}$ in the absence of the applied electric field as

$$\mathbf{I} = \mathbf{J}_0 - R_A(\mathbf{J}_0\cdot\mathbf{M})\mathbf{M} + \sigma R_0\mathbf{J}_0\times\mathbf{H}_i + \sigma R_1\mathbf{J}_0\times\mathbf{M}, \quad (2)$$

where $\mathbf{J}_0 = -R_A[\langle\mathbf{j}\times\mathbf{m}\rangle\times\mathbf{M} + \langle\mathbf{j}\cdot\mathbf{m}\rangle\mathbf{M}] + \sigma R_0\langle\mathbf{j}\times\mathbf{h}\rangle + \sigma R_1\langle\mathbf{j}\times\mathbf{m}\rangle$ is determined by the time average of the product of $\mathbf{j}$ and $\mathbf{m}$.

Equation (2) is the general expression for the spin rectification effect in FM. For materials with small AMR and Hall coefficients, the last three terms can be neglected, and Eq. (2) recovers an expression found earlier [15]. For devices with special geometry, the result can be further simplified. The geometric asymmetry of the spin dynamo shown in Fig. 1(d) leads to anisotropic electric and magnetodynamic responses. The eddy current is found flowing predominantly along the x axis, so that the dominant term of the spin-induced current is

$$I \approx -2R_A M_x\langle j_x m_x\rangle. \quad (3)$$

Since the components of $\mathbf{M}$ are described by the angles α, β, φ, and θ defined before, it is straightforward to show that, if $\beta = 0$, $I(\alpha, H) \approx -2R_A M_0[|H|/(|H| - M_0)]\langle j_x m_x\rangle\sin\alpha$ for $|H| > M_0$ and $I(\alpha, H) \approx -2R_A M_0\sqrt{1 - (H/M_0)^2}\langle j_x m_x\rangle(\alpha/|\alpha|)$ for $|H| < M_0$. When $\alpha = 0$, $I(\beta, H) = 0$ for $|H| > M_0$ and $I(\beta, H) \approx 2(R_A/N_y)\langle j_x m_y\rangle H\sin\beta$ for $|H| < M_1$. From these results, the bipolar symmetry deduced for $I(\alpha, H)$ and $I(\beta, H)$ is exactly the same as summarized in Eq. (1). The result $I(\beta, H) = 0$ for $|H| > M_0$ explains the disappearance of the sharp resonances in Figs. 2(c) and 2(d). Note that, for $|H| < M_1$, $I(\beta, H)$ is quasiresonant, which combines the resonant m_y and a linear dependence on H. It is easy to show that $|I(\beta, H)|$ saturates at about $2R_A\langle j_x m_y\rangle M_0$ at small angles, and $I(\beta, H)$ follows $\partial R(H)/\partial H$ in the field dependence, which explain the results shown in Figs. 2 and 3, respectively.

It is clear, therefore, that the spin rectification effect is analogous to the optical rectification effect. The effect appears whenever spin and charge responses mix via nonlinear responses. In semiconductors, spin-orbit coupling may affect such a mixing [3,4]. In FM, the effect is nonzero due to spin-charge coupling effects. It should be noted that a few earlier works [15,16] have analyzed in great detail weak dc effects induced by FMR in FM thin films, where a pulsed voltage signal was measured by using a high-power (up to kilowatts) pulsed microwave source. Here we measure directly dc currents with different characteristics: i.e., $I(\alpha, H)$ induced resonantly by both FMR and SSW and $I(\beta, H)$ caused quasiresonantly by the combination of AMR and spin excitations. An intriguing bipolar symmetry is revealed due to the microstrip geometry. Since a film has no in-plane preferential direction, the symmetry of dc effects in the film is much more cumbersome.

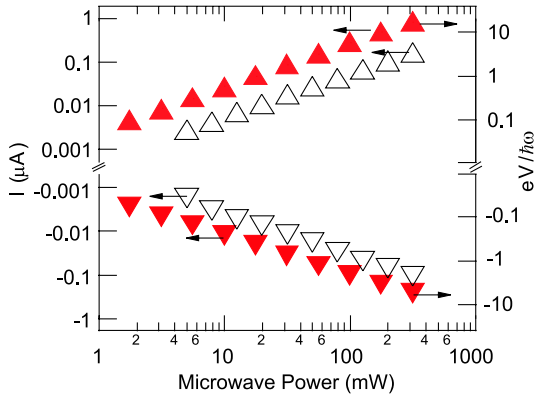

FIG. 4 (color online). The bipolar dc currents generated by both the FMR (upward triangles) and the $p = 2$ SSW (downward triangles) depend linearly on the microwave power. Open triangles are maximum currents measured at 5.4 GHz on a spin dynamo with the Py thickness $d = 137$ nm set at $\alpha = -1°$, $\beta = 0$. Solid triangles show both the closed circuit currents (left scale) and the open circuit voltages (right scale) measured at 6 GHz on a second spin dynamo with $d = 120$ nm set at $\alpha = -2°$, $\beta = 0$.

It follows from Eq. (2) that the spin-induced current and voltage are proportional to the microwave power. This is confirmed in Fig. 4, where the results for two spin dynamos measured over three decades of power range are plotted. Compared to earlier studies on semiconductors [3] and FM films [16], the current and voltage power sensitivity have been increased by 3 orders of magnitude, reaching values as high as 1 μA/W and 1 mV/W, respectively. To quantitatively evaluate the dc current enhancement, two additional experiments are performed to measure the amplitude of j_x and m_x. With an output microwave power of $P_0 =$ 316 mW at the frequency of 5.4 GHz, the amplitude of $j_x = 6.5$ mA is measured via the nonresonant resistance change induced by the bolometric effect [6], and the amplitude of $\mu_0 m_x = 20$ mT is determined by the precession cone angle extracted from the microwave-induced AMR change [7]. The large value of j_x indicates the high efficiency of the microwave power coupling between CPW and Py microstrips, which dissipates more than 10% of the microwave power P_0 in the Py microstrips via the charge dynamics. The large m_x indicates the high energy density of about 0.6 J/m^3 stored by the spin dynamics, which is about 200 times larger than that carried by the rf magnetic field in the proximity of the Py microstrip. These data explain the significant enhancement of the spin rectification effect. Using Eq. (3), the dc current is calculated to be $I = 0.27$ μA at $\alpha = -1°$ with $P_0 = 316$ mW, which agrees very well with the measured result shown in Fig. 4.

Finally, we compare the spin dynamo with the spin battery proposed recently [17,18]. In the spin battery, a dc voltage generated by FMR was predicted to occur via the spin pumping effect, with a universal high-power limit given by $eV/\hbar\omega \sim 1$. In contrast, $eV/\hbar\omega \sim 18$ is observed in Fig. 4 for the spin dynamo. We anticipate that the difference is caused by lateral spin transport in the spin dynamo, which was neglected for spin battery design based on interfacial spin pumping. Experimental efforts [7,8] have been made recently to test the spin battery. Since the characteristic length scale of the spin transport in FM is only about a few nanometers, one should be cautious in distinguishing dc effects caused by spin pumping and spin rectification. Precise angular-dependent measurement is essential. One should note that the dc signal generated by the spin rectification effect, as shown in Fig. 2, may reverse its sign and change the order of its magnitude by tilting the device through only a few tenths of a degree.

In summary, we have demonstrated a spin rectification effect which generates dc currents via spin wave excitations. The unprecedented high power sensitivity and the intriguing bipolar symmetry may enable new rf signal processing and sensor applications utilizing spin dynamics. A general and consistent view is achieved for interpreting spin-driven currents, which are currently of great interest and have been studied in a variety of materials.

We thank G. Roy and G. Mollard for technical assistance and D. Heitmann, U. Merkt, and DFG for the loan of equipment. N. M. is supported by the DAAD. This work has been funded by NSERC and URGP grants awarded to C.-M. H.

*Electronic addresses: hu@physics.umanitoba.ca
http://www.physics.umanitoba.ca/~hu

[1] A. A. Tulapurkar, *et al.*, Nature (London) **438**, 339 (2005).
[2] J. C. Sankey *et al.*, Phys. Rev. Lett. **96**, 227601 (2006).
[3] S. D. Ganichev *et al.*, Nature (London) **417**, 153 (2002).
[4] C. L. Yang *et al.*, Phys. Rev. Lett. **96**, 186605 (2006).
[5] C.-M. Hu *et al.*, Phys. Rev. B **67**, 201302(R) (2003).
[6] Y. S. Gui, S. Holland, N. Mecking, and C.-M. Hu, Phys. Rev. Lett. **95**, 056807 (2005).
[7] M. V. Costache *et al.*, Phys. Rev. Lett. **97**, 216603 (2006); Appl. Phys. Lett. **89**, 232115 (2006); J. Grollier *et al.*, J. Appl. Phys. **100**, 024316 (2006).
[8] A. Azevedo *et al.*, J. Appl. Phys. **97**, 10C715 (2005); E. Saitoh *et al.*, Appl. Phys. Lett. **88**, 182509 (2006).
[9] C. P. Wen, IEEE Trans. Microwave Theory Tech. **17**, 1087 (1969).
[10] A. H. Morrish, *The Physical Principles of Magnetism* (IEEE, New York, 2001).
[11] H. Puszkarski, Prog. Surf. Sci. **9**, 191 (1979).
[12] S. V. Vonsovskii, *Ferromagnetic Resonances* (Pergamon, New York, 1966), pp. 38–39; O. Mosendz *et al.*, J. Magn. Magn. Mater. **300**, 174 (2006).
[13] J. P. Jan, in *Solid State Physics*, edited by F. Seitz and D. Turnbull (Academic, New York, 1957), Vol. 5.
[14] S. Foner, Phys. Rev. **99**, 1079 (1955).
[15] H. J. Juretschke, J. Appl. Phys. **31**, 1401 (1960).
[16] W. G. Egan and H. J. Juretschke, J. Appl. Phys. **34**, 1477 (1963).
[17] A. Brataas *et al.*, Phys. Rev. B **66**, 060404(R) (2002).
[18] Y. Tserkovnyak *et al.*, Rev. Mod. Phys. **77**, 1375 (2005).